Turk J Phys
34 (2010) , 159 – 171.

doi:10.3906/fiz-1007-21

Role of quadrupole deformation in proton emitting nuclei in the medium mass region

Chandrasekaran Anu RADHA, Velayudham RAMASUBRAMANIAN and Emmanuel James Jebaseelan SAMUEL
Nuclear and Medical Physics Division, School of Advanced Sciences, VIT University, Vellore, 632014, Tamil Nadu-INDIA
e-mail: canuradha@vit.ac.in

Received 20.07.2010

Abstract

Nuclear structural studies at and beyond the proton drip line is done with the help of proton radioactivity. It is found that nuclei are not necessarily always spherical. The aim of the present work is to study the role of quadrupole deformation in proton rich nuclei, particularly with respect to odd Z nuclei within the region $50 < Z < 80$ near the proton drip line. The deformation is studied using triaxially deformed cranked Nilsson Strutinsky method with tuning. Some of the nuclei in the medium mass region are found to be proton emitters from the ground state with appreciable deformation. Nuclei with $62 < Z < 67$ shows considerable deformation that kindled the probability of instability within the nuclei. Significant ground state deformed shapes are observed in the $67 < Z < 73$ region.

Key Words: Proton radioactivity, quadrupole deformation, tuned cranked Nilsson Strutinsky shell correction method

1. Introduction

Various models and experiments are proposed to analyze the proton emitters in the region $Z = 50$ to 83, as it is very fertile for one proton radioactivity studies. Many nuclei in this region undergo proton decay from their ground state. Deformation of the nuclei exhibited in this region gives support for the nuclear structure studies far from stability. All known ground state proton emitters are odd Z since the unpaired proton is less bound and therefore lies closer to stability [1–3]. It is found that certain nuclei away from magic number shell closures exhibited collective modes of rotational excitation [4–6]. This indicates that nuclei have appreciable quadrupole moments and therefore could not be well described by the standard shell model which assumes a spherically symmetric nuclear shape. A self-consistent microscopic model introduced by Nilsson and Mottelson consists of a shell model for an ellipsoidal nucleus with one axis of symmetry using a deformed harmonic oscillator potential [7].

Proton emission is very sensitive to the decay energy available and so identification of possible candidates is influenced by proton separation energy predictions [8–11]. As more examples of proton emission have been

observed, this situation has been partially reversed and mass model predictions can be tested against known proton separation values [12–15]. The brief description for the formalism of triaxially deformed cranked Nilsson Strutinsky method which has been used for our results is given.

2. Theoretical formalisms

Quadrupole deformation is a basic phenomenon to study the shape transitions as well as radioactive nuclear process. Using the Nilsson wave function, it is possible to predict many important properties of odd Z nuclei as a function of deformation, such as magnetic and electric quadrupole moments, shape evolutions, pairing correlations etc. To evaluate the quadrupole deformation parameter, the formalism of our approach is very well known [16] so a brief account of the triaxially deformed cranked Nilsson Strutinsky method is discussed.

The first section gives the theoretical framework for obtaining quadrupole deformation values and energy calculation of the considered nuclei as a function of deformation β and nonaxiality γ parameters at different spins by the Strutinsky method. β vibrations are oscillations that preserve the axial symmetry of the deformed nucleus. The above two parameters, β and γ, define all possible quadrupole shapes, prolate, oblate and triaxial. The second section deals with the theoretical formalism involving the half-life calculation of the proton emitters based on Shanmugam-Kamalaharan model.

2.1. Triaxially deformed cranked Nilsson Strutinsky method

In nearly spherical nuclei, the coupling between the collective motion of the nucleons in the core and motion of the loose nucleons outside the core is weak. On the other hand, for strong coupling, the surface is distorted and the potential felt by the loose nucleons is not spherically symmetric. These nucleons, moving in a non-spherically symmetric shell model potential, maintains the deformed nuclear shape. For a non rotating nuclei (zero spin) shell energy calculations assumes a single particle field

$$H_0 = \Sigma h_0, \tag{1}$$

where h_0 is the triaxial Nilsson Hamiltonian given by

$$h_0 = \frac{p^2}{2m} + \frac{1}{2}m\sum_{i=1}^{3}\omega_i^2 x_i^2 + C\, l\cdot s + D\,\left(l^2 - 2\left\langle l^2\right\rangle\right). \tag{2}$$

By Hill-wheeler parameterization the three oscillator frequencies ω_i are given as

$$\omega_x = \omega_0 \exp\left(-\sqrt{\frac{5}{4\pi}}\beta\cos\left(\gamma - \frac{2}{3}\pi\right)\right)$$

$$\omega_y = \omega_0 \exp\left(-\sqrt{\frac{5}{4\pi}}\beta\cos\left(\gamma - \frac{4}{3}\pi\right)\right)$$

$$\text{and } \omega_z = \omega_0 \exp\left(-\sqrt{\frac{5}{4\pi}}\beta\cos\gamma\right),$$

with the constraint of constant volume for equipotentials:

$$\omega_x \omega_y \omega_z = \omega_0^3 = \text{constant}. \tag{3}$$

The values [11] for the Nilsson parameters κ and μ are chosen as

$$\kappa = 0.093 \,\text{and}\, \mu = 0.15.$$

The value for $\hbar\omega_0$ is taken as

$$\hbar\omega_0 = \frac{45.3\, MeV}{(A^{1/3} + 0.77)}. \tag{4}$$

The same values are used for both protons and neutrons. The factor 2 in front of $\langle l^2 \rangle$ in equation (2) has been used to obtain better agreement between the Strutinsky-smoothed moment of inertia and the rigid rotor value. The parameter D has been accordingly predetermined with the help of single particle levels in the indicated mass region. Using the matrix elements, the Hamiltonian is diagonalized in cylindrical representation up to $N = 11$ shells.

In a rotating nucleus ($I \neq 0$) without internal excitation, the nucleons move in a cranked Nilsson potential with the deformation described by β and γ. The cranking is performed around the Z-axis and the cranking frequency is ω. Thus, the Hamiltonian for a rotating case is given by

$$H_\omega = H_0 - \omega J_z = \sum h_\omega, \tag{5}$$

where

$$h_\omega = h_0 - \omega j_z. \tag{6}$$

Diagonalization of

$$\hbar_\omega \phi_i^\omega = e_i^\omega \phi_i^\omega \tag{7}$$

gives the single particle energy e_i^ω and wave function ϕ_i^ω. The single particle energy in the laboratory system and the spin projections are obtained as

$$\langle e_i \rangle = \langle \phi_i^\omega \,| h_\circ |\, \phi_i^\omega \rangle \,, \tag{8}$$

and

$$\langle m_i \rangle = \langle \phi_i^\omega \,| j_z |\, \phi_i^\omega \rangle \,. \tag{9}$$

The shell energy is given by

$$E_{sp} = \sum \langle \phi_i^\omega \,| h_\circ |\, \phi_i^\omega \rangle = \sum \langle e_i \rangle, \tag{10}$$

where

$$\langle e_i \rangle = e_i^\omega + \hbar\omega \, \langle m_i \rangle \,. \tag{11}$$

Thus,

$$E_{sp} = \sum e_i^\omega + \hbar\omega I, \tag{12}$$

with the total spin given by

$$I = \sum \langle m_i \rangle. \tag{13}$$

To overcome the difficulties encountered in the evaluation of total energy for large deformations through the summation of single particle energies, the Strutinsky shell correction method is adapted to $I \neq 0$ cases by suitably tuning [16, 17] the angular velocities to yield fixed spins. For unsmoothened single particle level distribution the spin I is given as

$$I = \int_{-\infty}^{\lambda} g_2 de^{\omega} = \sum_i \langle m_i \rangle \tag{14}$$

and

$$E_{sp} = \int_{-\infty}^{\lambda} g_1 e^{\omega} de^{\omega} + \hbar\omega I = \sum_i e_i^{\omega} + \hbar\omega I. \tag{15}$$

For the Strutinsky smeared single particle level distribution, equations (14) and (15) transform in to

$$\tilde{I} = \int_{-\infty}^{\lambda} \tilde{g}_2 de^{\omega} = \sum_i \langle \tilde{m}_i \rangle \tag{16}$$

and

$$\tilde{E}_{SP} = \int_{-\infty}^{\lambda} \tilde{g}_1 e^{\omega} de^{\omega} + \hbar\omega \tilde{I} \tag{17}$$

$$= \sum_i^N \tilde{e}_i^{\omega} + \hbar\omega \tilde{I}. \tag{18}$$

In the tuning method the total spin is adapted and is calculated as

$$I = \tilde{I}_z = \sum_{\nu=1}^{N} \left\langle \tilde{J}_z \right\rangle_{\nu}^{\omega} + \sum_{\pi=1}^{Z} \left\langle \tilde{J}_z \right\rangle_{\pi}^{\omega}. \tag{19}$$

For a chosen integer or half integer spins the above relation permits to select numerically the ω values. The calculations are repeated accordingly as the frequency values $\omega(I)$ change from one deformation point to another.

The total energy is given by

$$E_T = E_{RLDM} + \left(E_{sp} - \tilde{E}_{sp} \right), \tag{20}$$

where

$$E_{RLDM} = E_{LDM} - \frac{1}{2} I_{rig} \omega^2 + \hbar\omega \tilde{I}. \tag{21}$$

The liquid drop energy E_{LDM} is given by the sum of Coulomb and surface energies as

$$E_{LDM}(\beta, \gamma) = \left[2\chi (B_c - 1) a_s + (B_s - 1) \right], \tag{22}$$

where B_c and B_s are the relative Coulomb and surface energies of the nucleus. The values used for the parameters a_s and χ are $a_s = 19.7$ MeV and fissility parameter $\chi = (Z^2/A)/45$, where Z and A are the charge and mass numbers of the nucleus.

The rigid body moment of inertia I_{rig} is defined by β and γ, including the surface diffuseness correction, and $\tilde{I}$ is the Strutinsky smoothened spin [18]. For an ellipsoidal shape described by the deformation parameter $\beta$and shape parameterγ, the semi axes R_x,R_y,R_z are given by the relations

$$R_x = R_0 \exp\left[\sqrt{\frac{5}{4\pi}}\beta\cos\left(\gamma - \frac{2\pi}{3}\right)\right]$$

$$R_y = R_0 \exp\left[\sqrt{\frac{5}{4\pi}}\beta\cos\left(\gamma - \frac{4\pi}{3}\right)\right]$$

and $R_z = R_0 \exp\left[\sqrt{\frac{5}{4\pi}}\beta\cos\gamma\right]$.

By volume conservation, we have

$$R_x R_y R_z = (R_0^0)^3, \tag{23}$$

where R_0^0 is the radius of the spherical nucleus. Here,

$$R_0^0 = r_0 A^{1/3}\,(r_0 = 1.16\,fm)\,. \tag{24}$$

The moment of inertia about the Z axis is given by

$$\frac{I_{rig}\,(\beta,\gamma) + 2Mb^2}{\hbar^2} = \frac{1}{5}\frac{AM\left(R_x^2 + R_y^2\right)}{\hbar} + \frac{2Mb^2}{\hbar^2}, \tag{25}$$

where $2Mb^2$ is the diffuseness correction to the moment of inertia and the diffuseness parameter $b = 0.90$ fm [19–21].

The quadrupole deformations in the medium mass region isotopes have been obtained by the tuned Strutinsky procedure. In the calculation performed here the spin is varied from $I = 0\ \hbar$ to 30 $\hbar$ in steps of 2 $\hbar$, with zero temperature (0.0 MeV); γ from -180° to -120° in steps of 10°, and β from 0.0 to 0.8 in steps of 0.1. The Hill Wheeler expressions for the frequencies have been used in the cranked Nilsson model [7].

2.2. Single proton emission and half lives measurements

Experimental studies of proton rich nuclei involve the observation of ground state proton emission. The structure and decay modes of these nuclei beyond the dripline represent one of the most active areas of experimental and theoretical studies of exotic nuclei [21, 22]. In the last few years, many ground state and isomeric proton radioactivity have been reported in the region $51 < Z < 83$. The proton emitters are identified by calculating the separation energy values. In general, proton emission half-lives depend mainly on the proton separation energy and orbital angular momentum, but rather weakly on the details of the intrinsic structure of proton emitters, example, on the parameters of the proton-core potential [23, 24]. This suggests that the lifetimes of deformed proton emitters will provide direct information on the angular momentum content of the associated Nilsson state, and hence on the nuclear shape [25, 26]. The half lives of proton radioactivity are studied using Shanmugam-Kamalaharan model [21, 22].

A finite range Yukawa plus Exponential potential along with the Coulomb potential is used for the post scission region and a third order polynomial is used for the overlapping region. While the centrifugal barrier

has negligible role to play in cluster radioactivity, it becomes appreciable in the case of alpha decay. For proton emission the centrifugal effect should become very much considerable. Hence a centrifugal barrier is added to the post scission region for considering proton radioactivity.

The half-life of the meta-stable system is

$$T = \frac{\ln 2}{\nu P} \tag{26}$$

where

$$\nu = \frac{\omega}{2\pi} = \frac{E_\nu}{h} \tag{27}$$

represents the number of assaults on the barrier per second. That is the characteristic frequency of the collective model. The probability per unit time of penetration P through the barrier is

$$P = \frac{1}{1 + \exp K} \tag{28}$$

Substituting values of ν and P into T, we get

$$T = \frac{h \ln(1 + \exp K}{2E_\nu} \tag{29}$$

Expressing the time in seconds, the energies in MeV and the lengths in fm for the lifetime, one has

$$T = \frac{1.433 \times 10^{-21}(1 + \exp K)}{E_\nu} \tag{30}$$

The action integral K is given by

$$K = K_L + K_R \tag{31}$$

where

$$K_L = \frac{2}{\hbar} \int_{r_0}^{r_1} [2B_r(\nu)V(r)]^{1/2} dr \tag{32}$$

$$K_R = \frac{2}{\hbar} \int_{r_h}^{r_1} [2B_r(r)V(r)]^{1/2} dr \tag{33}$$

Here, K_L and K_R are the left and right integrals of the potential chosen. The limits of integration r_a and r_b are the two appropriate limits of the integral which are found by Newton-Raphson method. This method is applied first to calculate the life time T in seconds for the spontaneous emission of heavier fragments from certain actinide nuclei. The branching ratios are then obtained by using the experimental half-lives of the respective α disintegration.

The interaction potential is given by

$$V(r) = \frac{Z_1 Z_2 e^2}{r} + \frac{l(l+1)\hbar^2}{2B_r(\nu)r^2} + V_n(r) \tag{34}$$

where the first, second and third terms on the right hand side are the Coulomb, centrifugal and finite range potentials respectively. The centrifugal effect should become very much considerable. Hence a centrifugal barrier is added to the post-emission region for considering proton radioactivity.

The post-scission potential used by us incorporates the most important finite range effects in the calculations. Thus the proton when it is emitted from the contact point is greatly influenced by the finite range effects. Thus this turns out to be a new approach when compared with the other calculations. The nuclear inertia $B_r(r)$ is associated with the motion in the fission direction.

2.3. Calculation of single proton emission separation energy

The separation energy of the last proton is the energy required to separate one proton from a nucleus. The one proton separation energy is calculated using the relation

$$S_P(Z,N) = -M(Z,N) + M(Z-1,N) + m_P \tag{35}$$

The separation energies are calculated for the low and medium mass nuclei in the periodic table. The mass excess values for the nuclei are taken from Audi-Wapstra mass table [27]. The possible proton emitters are identified using this separation energy calculation as $S_p < 0$. Figure 1 shows the proton separation energy for different isotopes in the medium mass region. These nuclei are in a ready state to give out a proton enabling them to reach a stable configuration. The proton is emitted or removed from the nucleus with angular momentum. The spectroscopic factor which is the ratio of the experimental and theoretical half lives is calculated. The ratio between the actual and theoretical half life is indicative of the influence of structure effects such as the degree of parent and daughter wave functions overlap. Incomplete overlap is a hindrance to any decay which can only result in longer experimental half lives and hence to spectroscopic factors less than unity [12, 25].

It is found from Table the spectroscopic factor is greater than unity for $Ta^{156,157}$, $Re^{160,161}$ and Ir^{167}. It shows these nuclei are effective proton emitters.

3. Results and discussion

We have calculated the one proton separation energies, their half lives, ground state quadrupole deformation at the drip line and the corresponding spectroscopic factor. The calculated ground state quadrupole deformation of the nucleus in $56 < Z < 83$ is shown. The calculated values for one proton separation energy give the list of one proton emitters as they have Sp < 0. Generally the proton separation energy calculation helps in determining the magicity, shell closures and extrastability of the nuclides. Also they help in finding out the possible proton emitters as shown in Figure 1. The possible one-proton emitters are found to have an odd Z. In addition to be good proton emitters, odd Z nuclei are found to be more deformed than their even Z neighbours. This is due to the reason that pairing correlations are strongly reduced in odd Z nuclei and as a result the nucleus is driven towards larger deformation. Much stronger pairing in even Z nuclei results in almost spherical shapes. The relatively high potential barrier enables the observation of ground state proton radioactivity less possible in the region $Z \leq 50$.This is due to the low Coulomb barrier [26]. The half-lives of the possible proton emitters are calculated using SK model. The calculated values are compared with the experimental values reported in the literature.

In the Figure 1 the energy window provides the support for a direct observation of ground state proton emission which by principle is possible on the basis of calculated separation energies. The table includes the

Table. Experimental and calculated half lives and Quadrupole deformations of ground state proton emitters.

Nucleus	S_p (MeV)	β_2		LOG_{10} T (T in Sec)			Spectroscopic factor $T_{1/2}$(Theory) / $T_{1/2}$(Expt)
		Calculated	Moller &Nix [28]	Calculated	Expt.		
					[1,10,29,30]	[31]	
$^{109}I_{56}$	−.821	0.20	0.16	−4.4010	−4.0000	-	0.398
$^{112}Cs_{57}$	−.821	0.21	0.208	−3.5500	−3.3010	-	0.562
$^{113}Cs_{58}$	−.981	0.20	0.207	−5.6910	−4.7695	-	0.12
$^{146}Tm_{77}$	−1.1	−0.159	−0.199	−1.4130	−0.6289	-	0.1617
$^{147}Tm_{78}$	−1.05	−0.185	−0.190	−0.5420	0.4310	0.591	0.1064
$^{150}Lu_{79}$	−1.271	−0.11	−0.164	−2.4600	−1.3979	−1.180	0.0865
$^{151}Lu_{80}$	−1.24	−.05	−0.156	−2.1710	−0.8860	−0.896	0.051
$^{156}Ta_{83}$	−1.01	−.01	−0.053	−0.3970	−0.8416	−0.620	2.78
$^{157}Ta_{84}$	−.93	0.1	0.045	−0.4300	−0.5229	−0.523	1.24
$^{160}Re_{85}$	−1.2	0.05	0.080	−3.0570	−3.0604	−3.046	1.005
$^{161}Re_{86}$	−1.1	0.03	0.080	−2.7020	−3.4318	−3.432	5.369
$^{165}Ir_{88}$	−1.54	0.12	0.099	−4.9140	−3.4560	−3.469	0.0348
$^{166}Ir_{89}$	−1.15	0.15	0.107	−1.0790	−0.8180	−0.824	0.5480
$^{167}Ir_{90}$	−1.07	0.15	0.116	−0.3920	−0.9586	−0.959	3.686
$^{171}Au_{92}$	−1.45	−0.065	−0.105	−4.3640	−2.6536	−4.770	0.0194

one proton separation energy, ground state quadrupole deformation, the calculated half lives, experimental half lives from reference [27] and the corresponding spectroscopic factor.

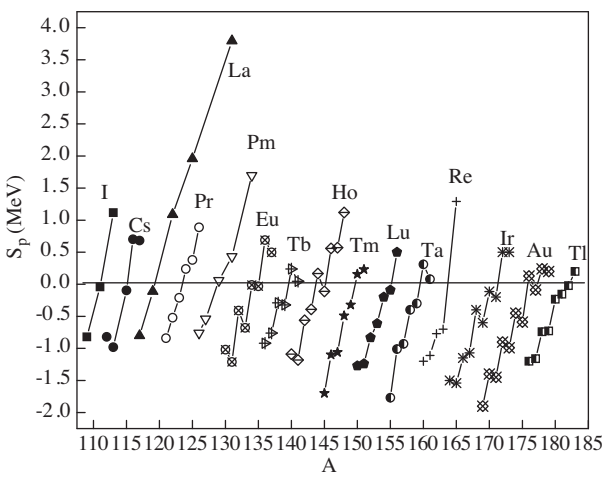

Figure 1. A plot of calculated single proton separation energy from the medium mass nuclei.

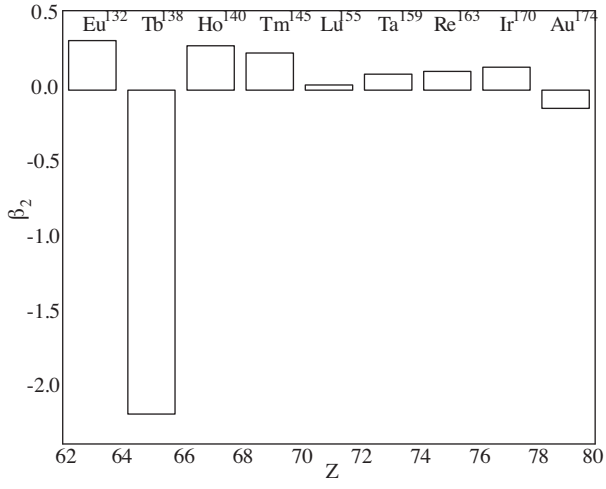

Figure 2. Calculated ground state quadrupole deformations for the nuclei in the $60 < Z < 80$ region.

For $Z > 67$, the nuclei is moderately deformed. Strong deformation is observed in $62 < Z < 67$. A shape transition is observed for Ho, Tm, Lu, Ta nuclei ($Z = 67, 69, 71, 73$). Re, Ir nuclei (Z = 75, 77) exhibit a moderate deformation. Au nucleus shows a strong oblate deformation. Figure 2 shows the calculated ground state quadrupole deformations of the last proton bound nuclei in the region $60 < Z < 80$ region. The oblate shape is found in the ^{138}Te and nuclei ^{132}Eu, ^{140}Ho, ^{145}Tm, ^{155}Lu, ^{159}Ta, ^{163}Re, ^{170}Ir and ^{174}Au are having normal prolate shapes in their ground state. In the deformed case, shell gaps occur at N and Z values that are different to the magic numbers for the spherical well.

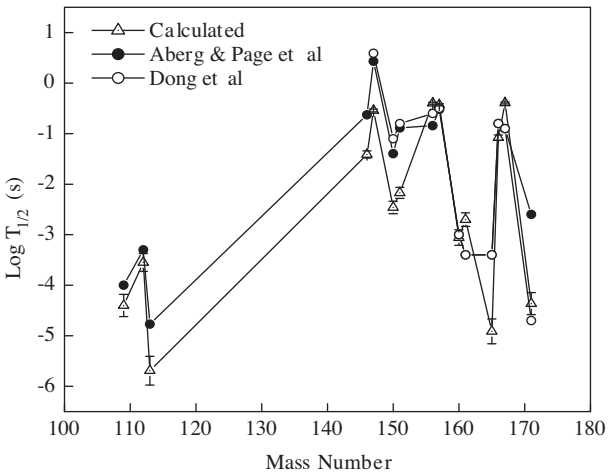

Figure 3. Calculated half lives of various nuclei are compared with different experimental values with error bars.

Figure 3 shows that the results of our half-lives calculations based on SK model agree fairly well with recent experimental data [31]. In general, proton emission half-lives depend mainly on the proton separation energy and orbital angular momentum, but rather weakly on the details of intrinsic structure of proton emitters However, our calculation reproduces the data for chosen nuclei with considerable accuracy.

For proton rich nuclei in the vicinity of medium mass region, Figure 4 displays data on deformation that are extracted from Moller and Nix calculations (solid circles), are compared with the present calculation (open circles). Our calculated deformation values are compared with the values of Moller-Nix et al. [28] and it is found that our values are in agreement with their values. The spherical shapes are found in the region $Z = 71$, 73 and 75. From the table, one could notice that normal deformations $\beta_2 = 0.10$ exist in the chosen mass region. It illustrates the quadrupole deformations of odd Z nuclei in the region $60 < Z < 80$. Significant quadrupole deformations are observed in the nuclei of $Z = 63$, 65 and 79. The variations in the calculated values of β, compared to Moller and Nix calculations, are found to be negligibly small. Both oblate and prolate quadrupole deformed shapes are observed in the chosen region. This suggests that the half-lives of deformed proton emitters will provide direct information on the angular momentum content of the associated Nilsson state, and hence, indirectly on the nuclear shape. This information kindles the structural determination of various nuclei in the chosen region. Since most of the nuclei represented in the Figure 4 are predicted to have a modest but nevertheless non-zero quadruple deformation $\beta \approx 0.15$, it was suspected that calculating the half-lives under the assumption that they had spherical shapes wouldn't work. The nuclei Eu^{130,131,132} and Ho^{140,141} are of special interest since they are found to be strongly deformed ($\beta \approx 0.3$).

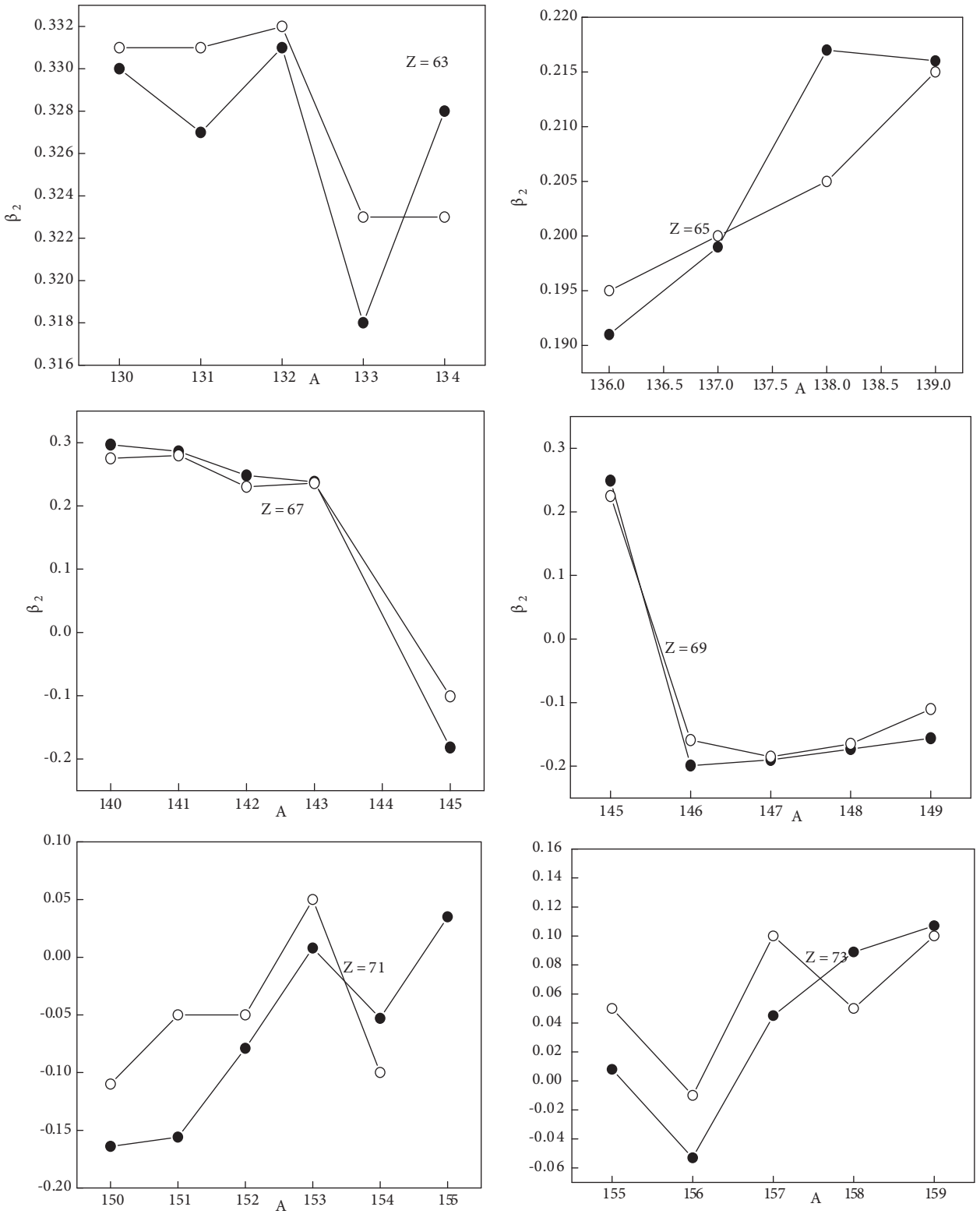

Figure 4. Quadrupole deformation of various nuclei in $60 < Z < 80$ region. The solid circle shows values from Moller and Nix [28] and hollow circle data are calculated from cranked Nilsson Strutinsky shell correction method [18].

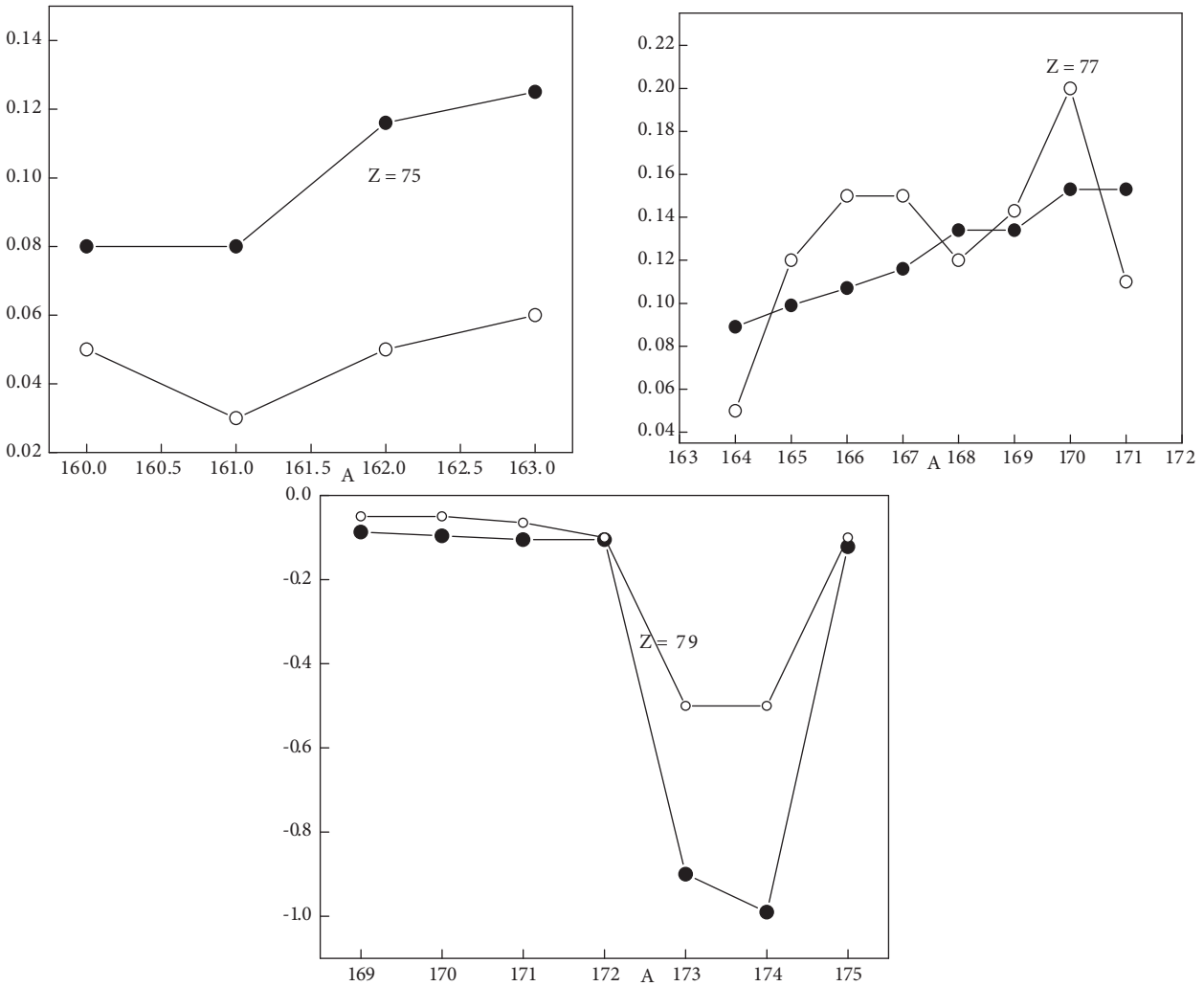

Figure 4. Continued

4. Summary and conclusion

In this work, we have analyzed the proton emitters in the region $57 < Z < 81$. We have used the SK model for our half life calculations which is essential for exotic nuclei with a realistic potential. We have identified the proton emitters using separation energy calculations. The even Z nuclei at the dripline are not accessible in experiments and we have compared the odd Z nuclei with Moller and Nix [28] values. We have calculated the corresponding spectroscopic factor and the quadrupole deformation is calculated using the cranked Nilsson Strutinsky method with tuning. Quadrupole deformation is a significant parameter which leads to radioactive decay by proton emission. Shape transitions observed in the $Z = 67, 69, 71, 73$ nuclei could be studied in future in a detailed way. The SK model and the cranked Nilsson Strutinsky shell correction method predicts the location of the proton drip-line, the ground-state quadrupole deformations, single proton separation energies at and beyond the drip-line, the deformed single-particle orbital occupied by the odd valence proton, and the corresponding spectroscopic factors. In conclusion, because of the microscopic shell correction method

and because of the reliability of the deformation diagrams employed in the calculations based on this method, it will appear to be useful in estimating deformations in the ground states of proton rich nuclei.

References

[1] S. Aberg, P. B. Semmes, W. Nazerwicz, *Phys. Rev.*, **C56,** (1997), 1762.

[2] G. A. Lalazissis, D. Vretenar, P. Ring, *Nuclear Physics,* **A650,** (1999), 133.

[3] G. A. Lalazissis, D. Vretenar, P. Ring, *Phys. Rev., **C**60,* (1999), 051302.

[4] S. B. Duarte, O. A. P. Tavares, F. Guzman, A. Dimarco, F. Garcia, O. Rodriguez, M. Goncalves, *Atomic Data and Nuclear Data Tables,* **80,** (2002), 235.

[5] D. Seweryniak, P. J. Woods, J. J. Ressler, C. N. David, A. Heinz, A. A. Sonzogni, J. Uusitalo, W. B. Walters, J. A. Caggiano, M. P. Carpenter, J. A. Cizewski, T. Davinson, K. Y. Ding, N. Fotiades, U. Garg, R. V. F. Janssen, T. L. Khoo, F. G. Kondev, T. Lauritsen, C. J. Lister, P. Reiter, J. Shergur, I. Wiedenhover, *Nuclear Physics*, **A682**, (2001), 247c.

[6] H. F. Zhang and G. Royer, *Phys. Rev.,* **C77**, (2008), 054318.

[7] S. G. Nilsson and I. Ragnarsson, S*hapes and Shells in Nuclear Structure,* (Cambridge University Press, Cambridge, England. 1995) p 50.

[8] T. Burvenich, K. Rutz, M. Bender, P. G. Reinhard, J. A. Maruhn, W. Greiner, *Eur. Phys. J.,* **A3**, (1998), 139.

[9] P. B. Semmes, *Nuclear Physics,* **A682,** (2001), 239c.

[10] D. T. Joss , I. G. Darby, R. D. Page, J. Uusitalo, S. Eeckhaudt , T. Grahn, P. T. Greenlees, P. M. Jones, R. Julin, S. Jutinen, S. Ketelhut, M. Leino, A.-P. Leppänen, M. Nyman, J. Pakarinen, P. Rahkil, J. Sarén, C. Scholey, A. Steer ,1, A. J. Cannon, P. D. Stevenson, J. S. Al-Khalili, S. Ertürk, M. Venhart, B. Gall, B. Hadinia, J. Simpson, *Physics Letters,* **B641,** (2006), 34.

[11] A. A. H. Mahmud, C. N. Davids, PJ. Woods, T. Davinson, A. Heinz, J. J. Ressler, K. Schmidt, D. Seweryniak, J. Shergur, A. A. Sonzogni, W. B. Walters, *Eur. Phys. J.,* **A15,** (2002), 85.

[12] A. A. Hassan Mahmud, PhD Thesis, Department of Physics and Astronomy, University of Edinburgh, UK, 2002.

[13] R. P. Rykaczewski, *Eur.Phys. J.,* **A15,** (2002), 81.

[14] D. S. Delion, R. J. Liotta, R. Wyss, *Physics Reports.,* **424,** (2006), 113.

[15] B. Blank, M. J. G. Borge, *Progress in Particle and Nuclear Physics.,* **60,** (2008), 403.

[16] C. Anu Radha and E. James Jebaseelan Samuel, *DAE-BRNS Proceedings of Int.Symp. on Nucl.Phys.,* **54**, (2009), 190.

[17] G. Shanmugam, Kalpana Sankar and K. Ramamurthi, *Phys. Rev.,* **C52,** (1995), 1443.

[18] G. Shanmugam, V. Ramasubramanian, S. N. Chintalapudi, *Phys. Rev.,* **C63,** (2001), 064311.

[19] G. Shanmugam and V. Selvam, *Phys. Rev.,* **C62**, (2000), 014302.

[20] G. Shanmugam, and B. Kamalaharan, *Phys. Rev.,* **C38**, (1988), 1377.

[21] G. Shanmugam, and B. Kamalaharan, *Phys. Rev.,* **C41**, (1990), 1742.

[22] G. Shanmugam, and B. Kamalaharan, *Phys. Rev.,* **C41**, (1990), 1184.

[23] G. Yuan, D. Jian-Min, Z. Hong Fei, Z. Wei, L. Jun-Qing, *Chinese Physics,* **C33**, (2009), 848.

[24] H. Y. Zhang, W. Q. Shen, Z. Z. Rent, Y. G. Ma, J. G. Chen, X. Z. Cai, C. Zhong, X. F. Zhou, Y. B. Wei, G. L. Ma, K. Wang, *Nuclear Physics,* **A722,** (2003), 518c.

[25] G. A. Lalazissis, D. Vretenar, P. Ring, *Nuclear Physics,* **A679,** (2001), 481.

[26] Lidia S. Ferriera, Miguel Costa Lopes, Enrico Maglione, *Progress in Particle and Nuclear Physics.,* **59,** (2007), 418.

[27] G. Audi, O. Bersillon, J. Blachot and A. H. Wapstra, *Nuclear Physics,* **A729,** (2003), 3.

[28] P. Moller, J. R. Nix, K. L. Kratz, *At. Data Nucl. Data Tables,* **66,** (1997), 131.

[29] D. N. Poenaru, *Nuclear decay modes*, (Institute of Physics Publishing, Bristol, 2003) 150.

[30] R. D. Page, L. Bianco, I. G. Draby, D. T. Joss, T. Grahn, R. D. Herzberg, J. Pakarinen, J. Thomson, S. Eeckhaudt, M. Leino, A.P. Leppanen, M. Nyman, P. Rahkila, J. Saren, C. Scholey, A. Steer, M. B. Gomez Hornillos, J. S. Al-Khalili, A. J. Cannon, P. D. Stevenson, S. Erturk, B. Gall, B. Hadinia, M. Venhart, J. Simpson, *Phys.Rev.,* **C75**, (2007), 061302.

[31] J. M. Dong, H. F. Zhang and G. Royer, *Phys. Rev.,* **C79**, (2009), 054330.